KFUPM
Journal of Undergraduate Research International

Diamond Open Access 18

Article Bioengineering

Spectral Investigation of AuNP Interactions with DNA-Functionalized U-Bent Optical Fiber Probes for EWA-Based Sensing

Fatimah Ali Aldoukhi and Tanzilur Rahman*

Cite https://doi.org/10.64589/juri/231565

Submitted: April 25, 2026 **Revised:** May 13, 2026 **Accepted:** May 15, 2026

ABSTRACT

This study systematically investigated the interfacial interaction between plasmonic gold nanoparticles (AuNPs) and oligonucleotide-functionalized U-bent plastic optical fibers (POFs) to understand electromagnetic coupling dynamics within the evanescent field, which is essential for evanescent wave absorbance (EWA)-based signal enhancement in optical fibers. U-bent POF probes were covalently conjugated with probe DNA *via* a wet-chemical amination protocol, and monodisperse citrate-capped AuNPs (50.1 nm, zeta potential -53.8 mV) were synthesized. Spectral analysis revealed that electrostatic interactions between the negatively charged AuNPs and the modified POF surface led to a localized surface plasmon resonance–mediated EWA enhancement, as evidenced by a significant reduction in light transmission and increased absorbance at 535 nm. However, stability assessments demonstrated weak interfacial binding, with the AuNPs readily detaching upon aqueous washing. Furthermore, although the probe POF exhibited target-specific DNA-capturing capabilities, subsequent AuNP interactions remained largely unspecific and structurally unstable. These findings highlight the critical necessity of engineering highly stable, site-specific conjugation strategies between plasmonic nanomaterials and bio-digital optical interfaces to realize robust, high-contrast signal amplification in next-generation optical fiber platforms.

Keywords: optical fibers, evanescent wave absorbance, gold nanoparticles, oligonucleotide, DNA targeting, surface interaction

1. INTRODUCTION

The integration of soft-matter waveguiding substrates with plasmonic nanomaterials has emerged as a robust framework for investigating nanoscale light-matter interactions, particularly in the development of advanced bio-digital interfaces[1,2]. Evanescent wave absorbance (EWA)-based platforms that leverage U-bent plastic optical fibers (POFs) are highly attractive owing to their structural flexibility, cost-effectiveness, and tunable sensing geometries[3,4]. These optoelectronic platforms frequently use gold nanoparticles (AuNPs) as signal amplifiers to achieve ultrasensitive signal modulation[5,6]. The extent of evanescent coupling is fundamentally governed by the nanometer-scale separation between the plasmonic elements and the waveguide boundary. When positioned within this high-intensity optical field, nanoparticles substantially enhance the extinction cross-section, driving a characteristic modulation of the localized surface plasmon resonance (LSPR)[7–9].

Despite the theoretical advantages of AuNP-mediated EWA enhancement, translating this phenomenon into reliable high-contrast diagnostics requires a comprehensive understanding of the interfacial binding dynamics between metallic nanoparticles and bio-functionalized optical fibers[10–13]. Specifically, the conjugation of probe oligonucleotides introduces complex electrostatic and steric variables that critically govern nanoparticle adsorption, spatial orientation, and sensing stability[14–16].

This study systematically evaluated surface interactions between biomolecule-functionalized U-bent POF probes and citrate-capped AuNPs using high-resolution spectral analyses. A bio-interface was fabricated using covalent DNA immobilization strategies, and dynamic binding with plasmonic nanoparticles was assessed in the absence and presence of specific target analytes (target and non-target DNAs). By quantifying light intensity attenuation and EWA enhancement along with rigorous washing protocols, this study elucidated the fundamental limitations of non-specific electrostatic nanoparticle adsorption. Ultimately, this study aimed to provide critical insights into the necessity of engineered, stable nanoparticle-fiber architectures for the realization of reproducible and highly specific EWA-based technologies.

2. EXPERIMENTAL SECTION

2.1. Materials. POFs consisting of polymethylmethacrylate (PMMA) as the core material (Refractive Index/RI = 1.49) and fluorinated polymer as the cladding (RI = 1.41) were purchased from Mitsubishi Rayon Pvt. Ltd., Japan. Gold (III) chloride, sodium citrate, citric acid, borate buffer, hexamethylenediamine (HMDA), glutaraldehyde, glycine, bovine serum albumin (BSA), and phosphate-buffered saline (PBS) were procured from Sigma-Aldrich, Saudi Arabia. All oligonucleotides (probe, target,

Published under an exclusive license by KFUPM

Table 1. *Material properties*

Oligonucleotide/ Name	Sequence
Probe	5'-TACTACCTCA[SP18][AmC6dT]
Target	5'-UGAGGUAGUAGGUUGUAUAGUU
Non-Target	5'-UAGCAGCACGUAAUAUUGGCG

and non-target DNAs) were obtained from IDT DNA Technologies, USA (Table 1).

2.2. Characterizations. Halogen light (HL2000, 350–1000 nm, Ocean Optics Inc., USA) was used as the light source for the optical measurements. The UV-Vis absorbance spectra of the optical fibers were measured using a high-resolution (HR) spectrometer (USB4000-XR1-ES, Ocean Optics Inc., USA). The light intensity of the optical fibers was further measured using a power meter (PM100USB, Thorlabs Inc., USA) equipped with fiber adaptors (BFT1, Thorlabs Inc., USA) and SMA connectors (B10510A, Thorlabs Inc., USA). The particle size and zeta potential were measured using a nanoparticle analyzer (Horiba Nanopartica SZ-100V2, Japan).

2.3. Synthesis of AuNPs. Monodisperse AuNPs with a nominal diameter of approximately 40 nm were synthesized using a modified citrate-reduction protocol based on a previous study[17]. To ensure high purity and eliminate extraneous nucleation sites, all glassware was pre-treated with aqua regia (HNO_3: HCl = 1:3 v/v) and rinsed thoroughly with deionized (DI) water. Briefly, 0.2 mL of 50 mM gold chloride solution ($HAuCl_4.3H_2O$) was diluted in 40 mL of DI water and brought to a vigorous boil under constant agitation. Subsequently, 0.65 mL of 17 mM trisodium citrate was rapidly added. The reaction was maintained until the solution exhibited a stable ruby-red hue, after which it was cooled to room temperature and stored at 4°. The resulting AuNPs were characterized using UV-Vis spectroscopy, exhibiting a characteristic LSPR peak at 535 nm with an optical density (OD) of 1.

2.4. Fabrication of U-bent POFs. U-bent POFs were fabricated using a glass-capillary-assisted thermomechanical process. Briefly, a 25 cm segment of POF (0.5 mm diameter) was conformed to a U-geometry by insertion into a 2 mm inner-diameter glass capillary. To achieve permanent structural deformation, the assembly was annealed at 100 °C for 10 min. The sensing region located at the apex of the U-bend was subsequently exposed by selective chemical de-cladding and meticulously cleaned using DI water and lint-free wipes. This process yielded probes with a 1.5 mm bend diameter and a 0.5 cm de-cladded sensing interface.

2.5. Surface Activation of POFs. To facilitate the covalent immobilization of the probe DNA, the PMMA fiber surfaces were chemically modified *via* a sequential wet-chemical protocol. The probes were cleaned with DI water and dried under a nitrogen stream. Surface amination was performed by incubating the fibers in a 10% (w/v) HMDA solution in 100 mM of borate buffer for 2 h, thereby introducing reactive primary amine moieties onto the PMMA backbone. Following rinsing with DI water, the fibers were thermally stabilized in a 45 °C oven for 10 min. To enable the subsequent coupling of the amine-modified probe DNA (DNA-NH_2), the aminated surfaces were activated through a 20 min incubation in 2.5% glutaraldehyde, which served as a bifunctional crosslinker. The modified probes were washed with DI water to remove residual reagents, yielding a stable, functionalized interface ready for biosensing applications.

2.6. Covalent Immobilization of Probe DNA onto the Surface-Activated POFs. The surface-activated U-bent sensing regions were incubated in 20 μl of 10 μM probe DNA for 3 h at room temperature to facilitate covalent attachment. A dual-step quenching and blocking protocol was employed to ensure high biosensing specificity. After rinsing with 1×PBS (pH 7.4), residual unreacted aldehyde groups were quenched by incubation in 20 mM glycine for 1 h. Subsequently, the probes were treated with 2 mg/mL isoelectric BSA in 0.1 M sodium citrate/citric acid buffer (pH 4.6) for 2 h. This step passivated the remaining non-functionalized surface voids, thereby minimizing non-specific target DNA adsorption. The bio-functionalized

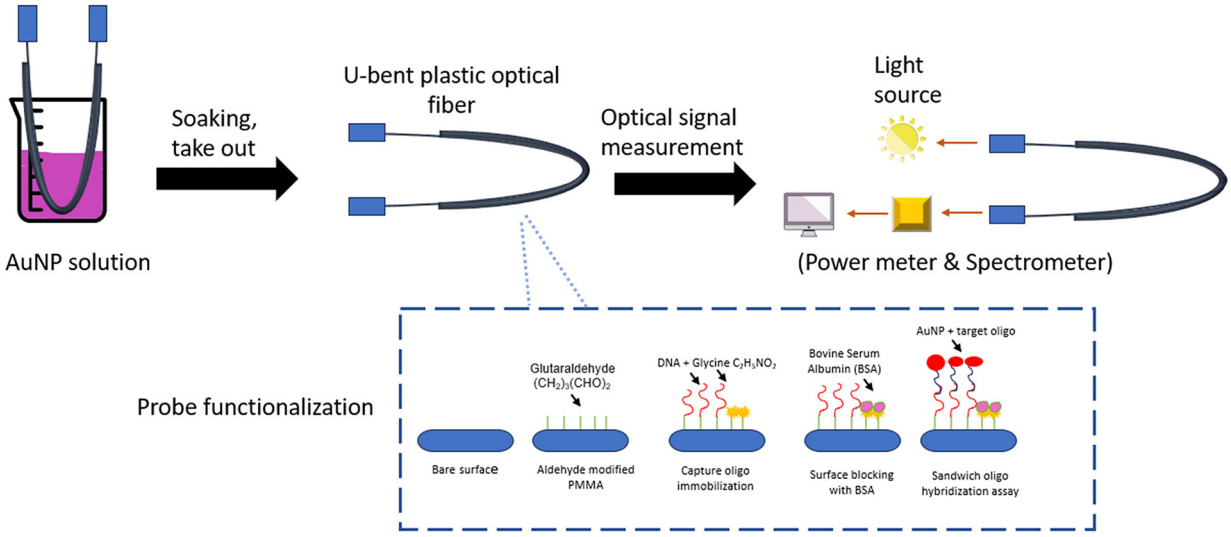

Figure 1. Schematic of POF functionalization with probe DNA and surface interaction investigation toward AuNPs and target and non-target DNA

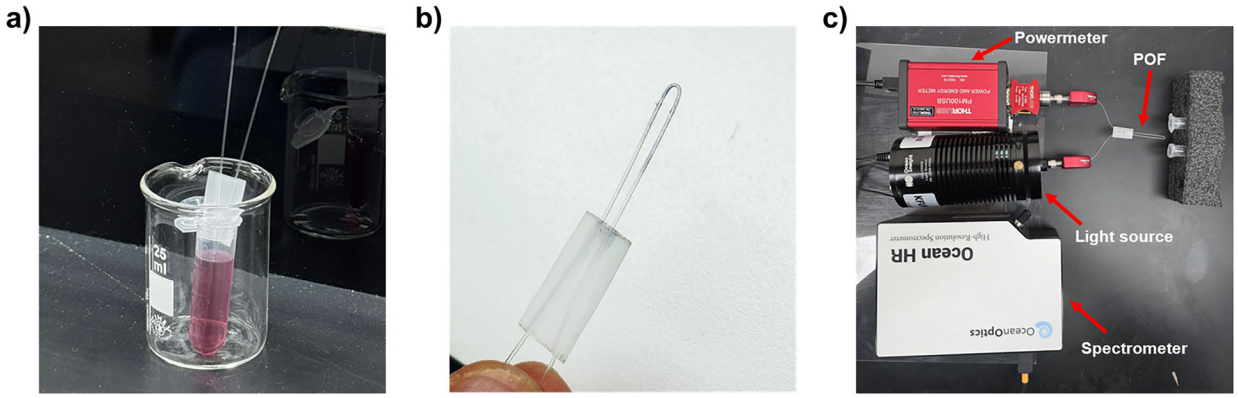

Figure 2. **a)** Ubent probe POF was immersed in the AuNP solution to allow surface interaction and nanoparticle adsorption. **b)** After 60 min of incubation in the AuNP solution, the POF surface showed visible modification, indicating attachment of AuNPs. **c)** POF device arrangement consisting of a power meter, halogen light source (350–1000 nm), and HR spectrometer

probes were finalized with sequential 1×PBS and DI water rinses to remove physisorbed species. The overall mechanism and conceptual design are illustrated in Figure 1.

2.7. Surface Interaction between the Probe POF and AuNPs in the Absence and Presence of Target and Non-Target DNA. The surface interaction between the probe POF and AuNPs was evaluated by immersing the sensing region of the probe POF in an AuNP solution (OD = 1) for different reaction times at room temperature. Changes in the absorbance and light intensity of the AuNP-incubated probe POF were measured using an HR spectrometer and a power meter. As a control, a bare POF was subjected to the same treatment as the probe POF. To assess the AuNP interaction with the probe POF in the presence of target and non-target DNA, the probe POF was initially treated with target or non-target DNA depending on the incubation time, followed by further time-dependent incubation with an AuNP solution prior to absorbance and light intensity measurements using an HR spectrometer and a power meter. To evaluate the binding strength of the AuNPs on the probe POF surface, the post-incubated probe POF was thoroughly washed with DI water, and the absorbance and light intensity were measured. The experimental setup is illustrated in Figure 2a–c.

3. RESULTS AND DISCUSSION

3.1. Assessing the Surface Interaction between AuNPs and the Probe POF. The evaluation of interfacial interactions between AuNPs and oligonucleotide-modified POFs (the probe POF) is fundamental to understanding the coupling dynamics within the EWA field. The proximity of these plasmonic nanostructures to the fiber interface dictates the efficiency of evanescent-wave interaction, where a high local field intensity triggers a significant enhancement of the extinction cross-section and can induce shifts in the LSPR, thereby maximizing absorbance modulation. This synergistic integration of AuNPs with a waveguiding fiber substrate offers a robust framework for investigating nanoscale light-matter interactions. While conjugated probe DNA provides high affinity toward target DNA owing to sequence-specific binding, the AuNP–probe POF interaction provides significant advantages, including the ability to achieve high-contrast signal amplification and tailored spectral responses, which are essential for developing advanced bio-digital interfaces and integrated optoelectronic platforms.

The fabricated probe POF was initially characterized by measuring the light intensity between the bare POF (before probe-DNA conjugation) and the probe POF (after oligo–probe conjugation) using a power meter. As shown in Figure 3a, the light

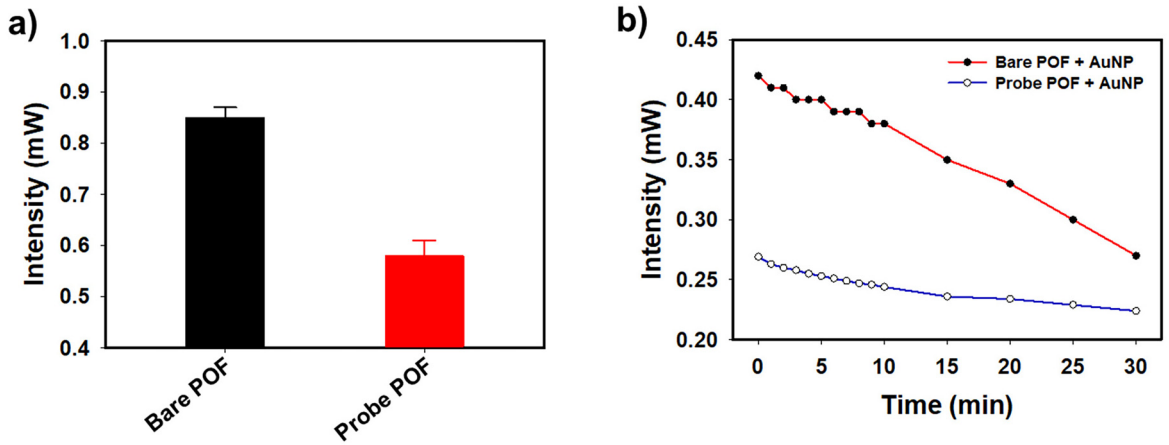

Figure 3. Light intensity measurements of bare and probe POFs: **a)** before incubation with an AuNP solution and **b)** after incubation with an AuNP solution as a function of the reaction time (0–30 min)

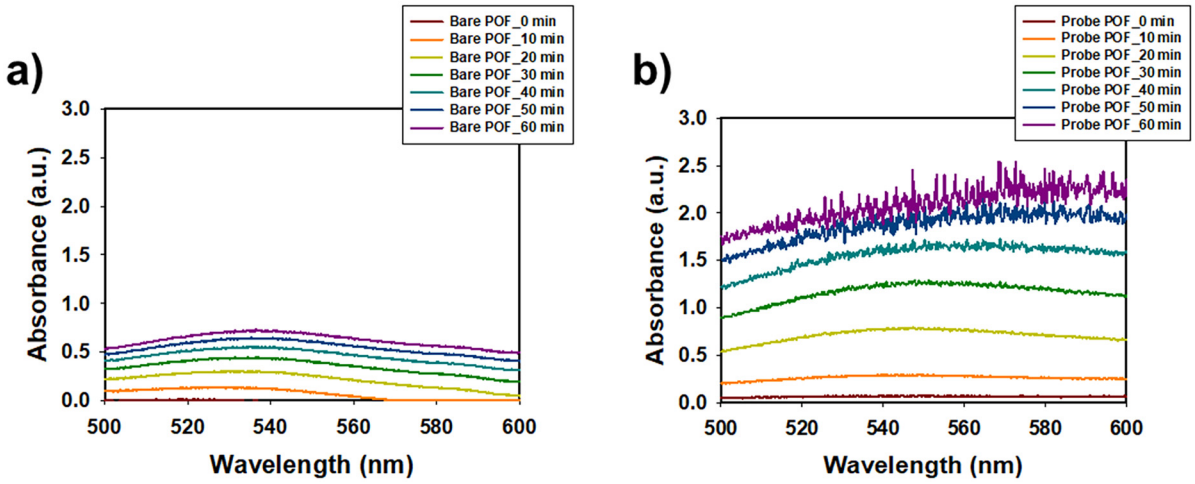

Figure 4. UV-Vis absorbances of **a)** bare POF and **b)** probe POF after incubation with an AuNP solution depending on the reaction time (0–60 min). λ_{abs} of AuNPs was 535 nm

intensity of the probe POF was 0.583 mW, which is significantly lower than that of the bare POF (0.841 mW). This decrease in light intensity indicated a change in the POF surface structure after conjugation of the probe DNA, revealing the successful functionalization of the POF using the probe DNA. The probe and bare POFs were further incubated with the AuNP solution to study their interactions with the LSPR-type nanoparticles. Time-dependent incubation in AuNP solution (0–30 min) showed a decrease in light intensity over time for both POFs, with the probe POF exhibiting a lower light intensity than the bare POF (Figure 3b). The decrease in light intensity of the POFs, particularly in the probe POF, revealed the attachment of AuNPs on the surface of the POF, which enhanced the EWA within the POF and resulted in a significant decrease in light intensity.

This EWA mechanism was confirmed by the HR spectroscopy data of the bare and probe POFs during time-dependent incubation (0–60 min) with AuNPs (Figure 4). The absorbance peak of the AuNPs was observed at 535 nm for both POFs, and gradually increased with longer incubation times. The absorbance of the probe POF (Figure 4b) was higher than that of the bare POF (Figure 4a). These data confirm the attachment of AuNPs to the surface of the POFs, with stronger interaction observed for the probe POF. The stronger interaction between the probe POF and AuNPs was due to electrostatic interactions between the highly negative surface charge of AuNPs and probe DNA, as the AuNPs were capped with abundant citrate groups and probe DNA contained terminal amine groups[18–20]. To confirm this, the synthesized AuNPs used for this experiment were characterized using dynamic light scattering (DLS) to determine the average particle size and a zeta potential analyzer to determine the nanoparticle surface charge. The particle size of the as-synthesized AuNPs was found to be 50.1 nm, similar to that of typical AuNPs reported elsewhere (Figure 5a). Furthermore, zeta potential measurement showed a highly negative surface charge of the AuNPs (-53.8 mV), proving that the electrostatic interaction can occur with positive charge-bearing amine modified probe DNA (Figure 5b).

The stability of the surface interaction between AuNPs and probe POF was also evaluated to understand the binding strength of AuNPs to the probe POF surface, which defines whether the attachment of AuNPs is strong or weak. To assess the stability of the AuNPs attached to the probe POF, the post-incubation probe POF with AuNPs was soaked in water for 30 min, and the absorbance of the probe POF was reevaluated. As shown in the HR spectroscopy results in Figure 6, the large gap between the absorbance peaks of the AuNP-treated probe POF before and

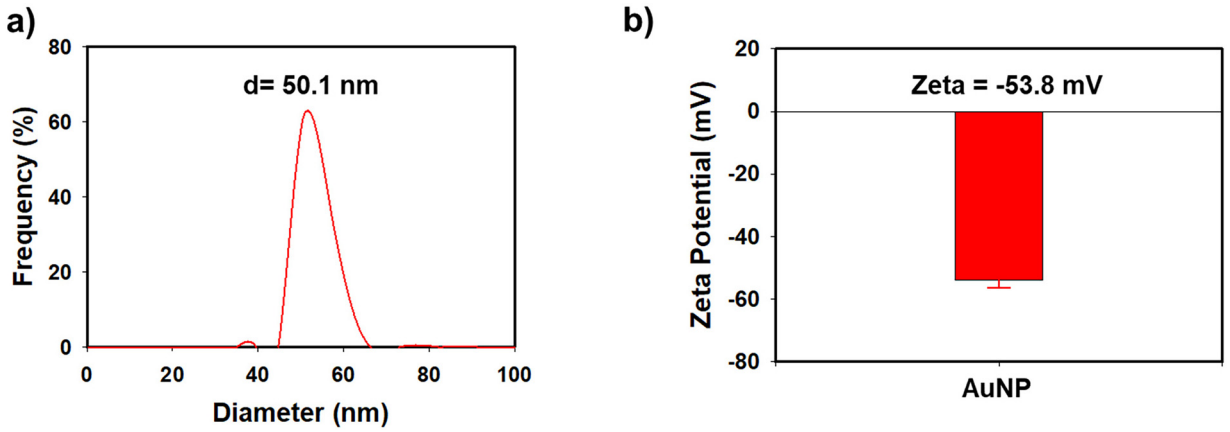

Figure 5. **a)** Particle size analysis using DLS, and **b)** Zeta potential (surface charge) of AuNPs

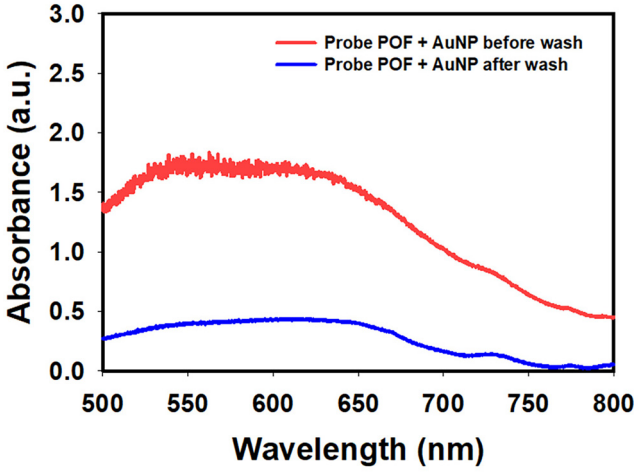

Figure 6. UV-Vis absorbances of the probe POF post-incubation with AuNP after washing with water to assess the surface attachment stability of AuNPs

after washing with water indicated a substantial change in the AuNP–probe POF surface interaction. The absorbance of the AuNP-treated probe POF dramatically decreased owing to the detachment of the AuNPs, which reduced the effect of EWA on the probe POF. This phenomenon revealed that although AuNP binding occurred at the probe POF surface, the degree of binding tended to be weak, as the AuNPs were easily washed away from the surface. This finding suggests that further modification of the AuNPs or probe POF surfaces is necessary to achieve more stable binding and interactions, which is beneficial for EWA enhancement in the probe POF.

3.2. AuNPs and Probe POF Interaction in the Presence of Target and Non-Target DNA. The conjugated probe DNA on the POF surface was designed using specific oligonucleotide sequences that matched the desired target DNA. Hence, the probe POF can capture the target DNA and change its surface to influence its interaction with the AuNPs. To confirm this hypothesis, the probe POF was exposed to the target DNA solution to facilitate binding before further interaction with AuNPs. For validation, non-target DNA was used to provide clearer insight into the DNA-capturing behavior of the probe POF. As shown in Figure 7a–b, a distinct light intensity was recorded between probe POF incubated with target DNA and that incubated with non-target DNA. The light intensity of the target DNA-treated probe POF was remarkably higher (0.283 mW) than that of the non-target DNA-treated probe POF (0.259 mW), with a gradual increase in light intensity over time, whereas the light intensity of the non-target-treated probe POF was unchanged. These data confirm the distinct binding phenomenon between the target and non-target DNAs, which is closely correlated with the specific DNA sequences between the probe and the target.

The investigation was further extended to the probe POF in the presence of target and non-target DNA and AuNPs by incubation and subsequent exposure to the AuNP solution. Power meter measurements showed distinct light intensities between the AuNP-target-probe POF and the AuNP-non-target-probe POF, followed by a time-dependent decrease in light intensity for both samples (Figure 8a). Furthermore, the UV-Vis spectra of both probe POFs revealed that washing with water after AuNP incubation reduced the absorbance of the probe POFs owing to the detachment of AuNPs from their surface (Figure 8b–c). These data confirm the non-specific binding of AuNPs to the probe POF in the presence of target and non-target DNA. The results demonstrated that although the presence of AuNPs on the surface of the probe POF can enhance EWA, more stable and specific binding of AuNPs is required to achieve a consistent and stable enhanced signal from the EWA phenomenon.

4. CONCLUSIONS

This study comprehensively evaluated the interfacial coupling dynamics between AuNPs and oligonucleotide-functionalized U-bent POF probes. While spectral analysis confirmed that the presence of AuNPs on the POF surface significantly enhances EWA and attenuates transmitted light intensity, this interaction is primarily driven by electrostatic affinity between the highly negative AuNPs (-53.8 mV) and the functionalized probe interface. Consequently, the resulting nanoparticle-fiber binding

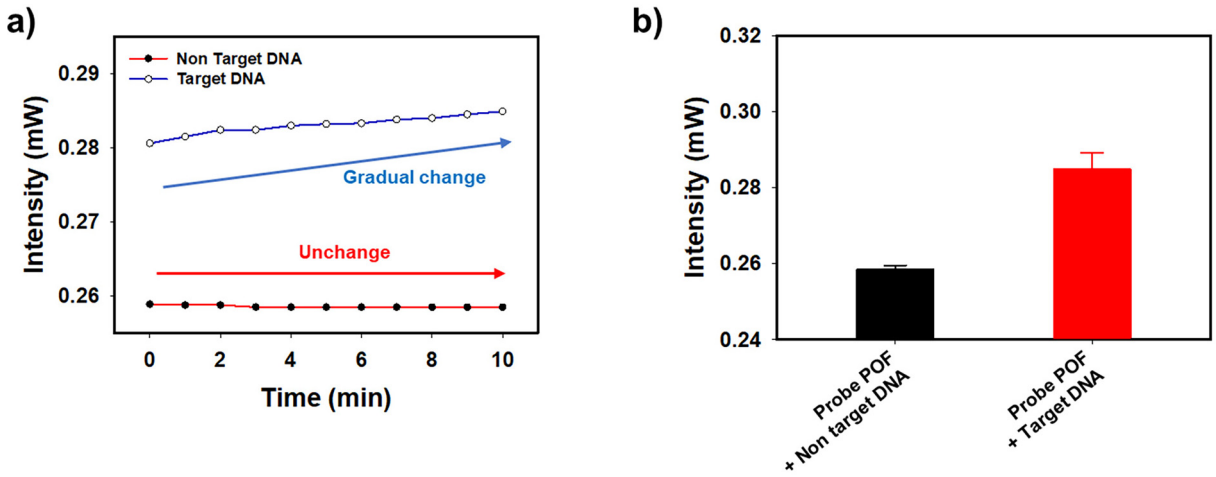

Figure 7. **a)** Binding responses of the probe POF toward target and non-target DNA depending on the incubation time, **b)** Light intensity of the probe POF after incubation with target and non-target DNA for 10 min

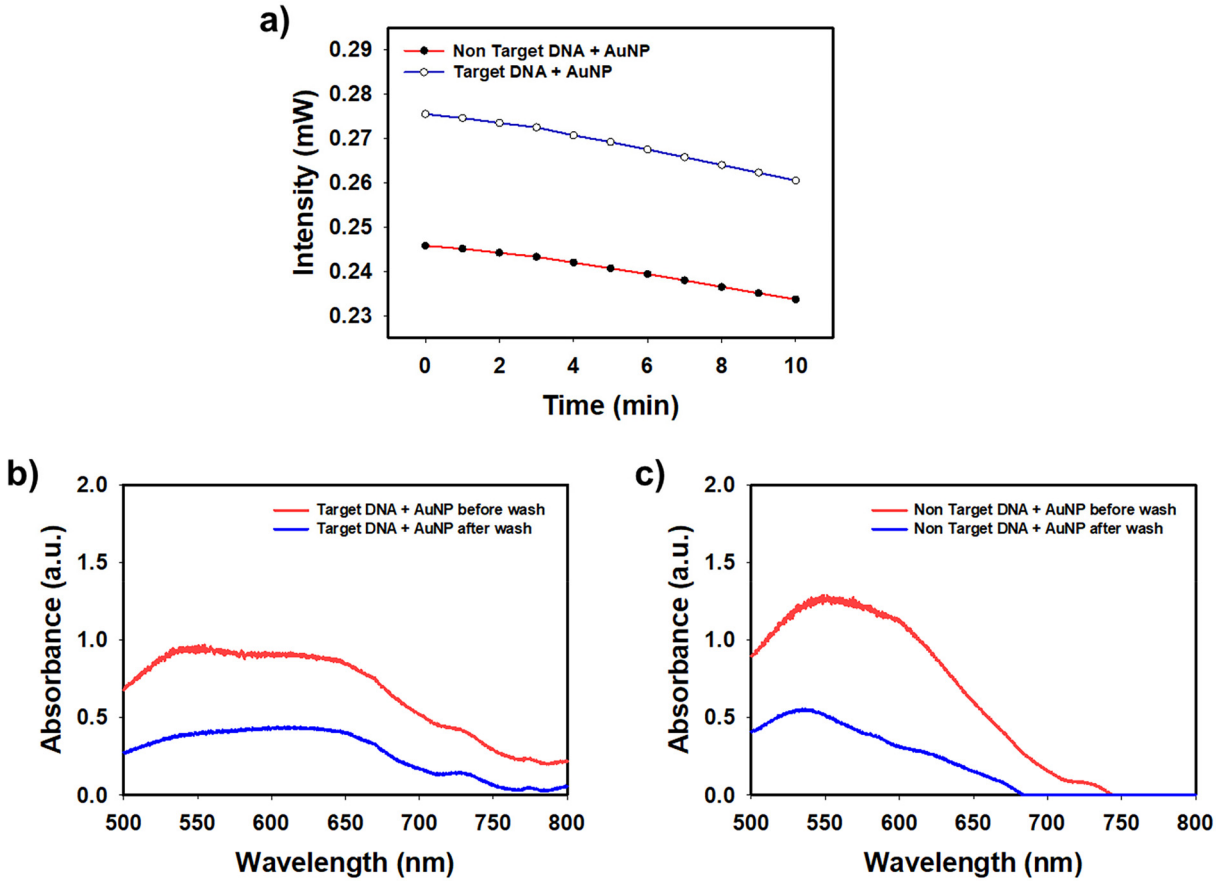

Figure 8. **a)** Light intensity of the probe POF after incubation with target and non-target DNA (10 min), followed by time-dependent incubation with an AuNP solution. **b)** UV-Vis absorbances of the probe POF post-incubation with target and non-target DNA and AuNPs after washing with water

exhibited pronounced instability, with significant AuNP detachment occurring upon exposure to simple aqueous washing. Furthermore, although the POF probes successfully demonstrated specific target DNA hybridization, subsequent non-specific AuNP adsorption failed to provide a reliable or structurally stable signal amplification mechanism. These findings underscore the critical design challenge in the fabrication of plasmonically enhanced optical fibers. Relying solely on electrostatic or non-specific interfacial interactions is insufficient to achieve robust optoelectronic device performance. To fully harness the advantages of high-contrast signal amplification and tailored spectral responses in bio-digital interfaces, future research must prioritize the development of engineered stable conjugation chemistries, such as functionalizing AuNPs with target-specific probe DNA. Establishing robust site-specific binding mechanisms between the target analyte and plasmonic enhancers is essential for translating these dynamic light-matter interactions into a reliable EWA-based optical fiber platform.

AFFILIATIONS AND AUTHOR DETAILS

Undergraduate Author

Fatimah Ali Aldoukhi – *Bioengineering Department, King Fahd University of Petroleum & Minerals, Dhahran 31261, Saudi Arabia* 0009-0003-4582-5495
Email: s202344170@kfupm.edu.sa

Corresponding Author

Tanzilur Rahman – *Research Mentor, Bioengineering Department, King Fahd University of Petroleum & Minerals, Dhahran 31261, Saudi Arabia* 0000-0002-9638-4824
Email: tanzilur.rahman@kfupm.edu.sa

ACKNOWLEDGMENTS

The authors acknowledge the support of Dr. Akhmad Irhas Robby, Postdoc, KFUPM who performed experiments as well as prepared the manuscript. Authors are thankful to the Department of Bioengineering and the Interdisciplinary Research Center for Biosystems and Engineering at King Fahd University of Petroleum and Minerals for the research support. This research was funded by Project Nos. INBS2509 and INBS2512.

REFERENCES

(1) Zhou, H., Li, D., Wang, Y. & Lee, C. Plasmonic metamaterials for multi-effect enhancement: bridging optical, electronic, thermal, and acoustic domains. *npj Metamaterials* **2**, 14 (2026).

(2) Fu, Y., Qing, Y. M., Li, Z., Zayats, A. V. & Lei, D. Tale of Two Resonances: Waveguide–Plasmon Coupling and High Q -Factor Engineering on the Nanoscale. *ACS Photonics* **10**, 2–12 (2023).

(3) Awad, O., Ghannoum, A. & Nieva, P. Harnessing the Unique Nature of Evanescent Waves: Optimizing FOEW LSPR Sensors with Absorption-Focused Nanoparticle Design. *Fibers* **13**, 81 (2025).

(4) Ramakrishna, B. & Sai, V. V. R. Evanescent wave absorbance based U-bent fiber probe for immunobiosensor with gold nanoparticle labels. *Sens. Actuators B Chem.* **226**, 184–190 (2016).

(5) Karnwal, A. *et al.* Gold Nanoparticles in Nanobiotechnology: From Synthesis to Biosensing Applications. *ACS Omega* **9**, 29966–29982 (2024).

(6) Kumalasari, M. R., Alfanaar, R. & Andreani, A. S. Gold nanoparticles (AuNPs): A versatile material for biosensor application. *Talanta Open* **9**, 100327 (2024).

(7) Lapointe, J., Grégoire, A., Bérubé, J.-P. & Vallée, R. Enhancing Evanescent Wave Coupling of Near-Surface Waveguides with Plasmonic Nanoparticles. *Sensors* **23**, 3945 (2023).

(8) Wang, B. *et al.* High-Q Plasmonic Resonances: Fundamentals and Applications. *Adv. Opt. Mater.* **9**, (2021).

(9) dos Santos, P. S. S. *et al.* From localized to propagating surface plasmon resonances in Au nanoparticle-coated optical fiber sensors and its implications in biosensing. *Photonics Res.* **12**, 2166 (2024).

(10) Cordeiro, M., Ferreira Carlos, F., Pedrosa, P., Lopez, A. & Baptista, P. Gold Nanoparticles for Diagnostics: Advances towards Points of Care. *Diagnostics* **6**, 43 (2016).

(11) Bouché, M. *et al.* Recent Advances in Molecular Imaging with Gold Nanoparticles. *Bioconjug. Chem.* **31**, 303–314 (2020).

(12) Colapietro, P., Brunetti, G., Panciera, C., Elicio, A. & Ciminelli, C. Shining the Path of Precision Diagnostic: Advancements in Photonic Sensors for Liquid Biopsy. *Biosensors (Basel).* **15**, 473 (2025).

(13) Arcos Rosero, W. A., Bueno Barbezan, A., Daruich de Souza, C. & Chuery Martins Rostelato, M. E. Review of Advances in Coating and Functionalization of Gold Nanoparticles: From Theory to Biomedical Application. *Pharmaceutics* **16**, 255 (2024).

(14) Kant, K. *et al.* Plasmonic nanoparticle sensors: current progress, challenges, and future prospects. *Nanoscale Horiz.* **9**, 2085–2166 (2024).

(15) Dougan, J. A., Karlsson, C., Smith, W. E. & Graham, D. Enhanced oligonucleotide-nanoparticle conjugate stability using thioctic acid modified oligonucleotides. *Nucleic Acids Res.* **35**, 3668–3675 (2007).

(16) Thakur, S., Cavallini, N., Ferrari, D. & Fabris, L. Interaction of Oligonucleotides with Gold Nanoparticles: Factors Beyond Electrostatic and Van-Der Waals Forces. *Adv. Mater. Interfaces* **12**, (2025).

(17) Sai, V. V. R., Kundu, T. & Mukherji, S. Novel U-bent fiber optic probe for localized surface plasmon resonance based biosensor. *Biosens. Bioelectron.* **24**, 2804–2809 (2009).

(18) Wei, X., Alam, A. R., Mo, Q. & Hernandez, R. Structure and Zeta Potential of Gold Nanoparticles with Coronas of Varying Size and Composition. *The Journal of Physical Chemistry C* **129**, 4204–4214 (2025).

(19) Wei, X., Popov, A. & Hernandez, R. Electric Potential of Citrate-Capped Gold Nanoparticles Is Affected by Poly(allylamine hydrochloride) and Salt Concentration. *ACS Appl. Mater. Interfaces* **14**, 12538–12550 (2022).

(20) Nial, P. S. & Subudhi, U. Zeta potential of Z-DNA: A new signature to study B-Z transition in linear and branched DNA. *Int. J. Biol. Macromol.* **266**, 131238 (2024).